

Electrical conducting properties of Na₂Zn₂TeO₆ thick films fabricated by aerosol deposition

Shusaku Teshima, Yuki Ono, Norimasa Goto, Ryoji Inada*

Department of Electrical and Electronic Information Engineering, Toyohashi University of Technology,
1-1 Hibarigaoka, Tempaku-cho, Toyohashi, Aichi 441-8580, Japan.

*Corresponding author:

Phone: +81-532-44-6723, Fax: +81-532-44-6757, E-mail address: inada.ryoji.qr@tut.jp

Abstract

We fabricated Na₂Zn₂TeO₆ (NZTO) ceramic electrolyte thick films by aerosol deposition (AD) method without applying any thermal treatment. Ball-milled NZTO powders are directly splayed onto a metallic substrate to form the thick film via impact consolidation phenomena at room temperature. NZTO film formed by AD has a thickness of 25 μm and an identical crystal structure with base powder. Ionic conductivity of as-deposited NZTO thick film was estimated to be $0.74 \times 10^{-5} \text{ S cm}^{-1}$ at room temperature. On the contrary, electronic conductivity of the film was four orders lower than the ionic conductivity. Although the ionic conductivity of as-deposited NZTO film by AD is more than one order of magnitude lower than that of sintered NZTO, obtained electrical conducting property is acceptable level for thin film sodium-ion battery application.

Keywords: honeycomb layered oxide, thick film, aerosol deposition, sodium-ion conductivity

1. Introduction

Na ion conducting layered oxide Na₂Zn₂TeO₆ (NZTO) is an attracted solid electrolyte material for the application to all-solid-state sodium-ion batteries (SiBs), because of the high ionic conductivity above $10^{-4} \text{ S cm}^{-1}$ at room temperature range and excellent chemical and electrochemical stability [1–5]. NZTO has a honeycomb-structured compound with a space group of *P6₃22* and in the layers, every TeO₆ octahedron is surrounded by six ZnO₆ octahedra via edge-sharing [2, 3]. Na ions are located between the layers at three different sites, all of which are partially occupied and Na ions can migrate among them.

The sintering temperature for densification of NZTO is 800–900 °C [1–5] and much lower than that for other Na-ion conducting oxide such as Na-β/β' alumina [6, 7] and Na₃Zr₂Si₂PO₁₂ [8, 9]. However, the

densification temperature of NZTO may be still high for the formation of good solid-solid interface with most electrode active materials through co-sintering process. The decreasing the densification temperature is strongly required for fabricating ceramic-based all-solid-state SiBs. In addition, thinner thickness of a solid electrolyte layer in a solid-state SiB is favorable for enhancing the volumetric energy density.

In this work, we applied the aerosol deposition (AD) method for fabricating NZTO thick film for the first time, which uses impact consolidation for ceramic particles at room temperature [10, 11]. Although the ratio of the amount of powder that contributed to film formation to the amount of base powder used is low, the film formed by AD has similar structural and physical properties as the base powder material. Based on this feature, the applicability of AD process for Li-ion conducting solid electrolyte thick films have been already reported [12–15]. Microstructure and electrical conductivity of as-deposited NZTO films were investigated for the feasibility of AD for fabricating Na-ion conducting ceramic thick films.

2. Experimental

NZTO thick films were formed on a SUS316L substrate by AD process with NZTO powder synthesized by a solid state reaction method. Primary parameters for film fabrication are summarized in Table 1. Crystal phase and microstructure were investigated by X-ray diffraction (XRD) analysis and scanning electron microscopy (SEM). The electrical conductivity of an as-deposited film was characterized using AC impedance and DC polarization measurements. The details are described in Supplemental data.

3. Results and discussion

SEM images for ball-milled NZTO powder used for film fabrication and as-deposited NZTO thick film are shown in Fig. 1(a)–(c). The size and morphology of ball-milled NZTO particles are not uniform. As-deposited NZTO film is composed of sub-micrometer sized NZTO particles and the film thickness is approximately 25 μm . The relative density of NZTO film is calculated by the theoretical density of NZTO ($= 4.88 \text{ g cm}^{-3}$), the deposition area size (1 cm^2), thickness ($= 25 \mu\text{m}$) and mass ($= 8 \text{ mg}$) of the film and estimated to be approximately 70 %, which is lower than sintered NZTO ($= 85 \%$) confirmed in our previous works [4, 5]. The X-ray diffraction patterns for NZTO base powder and NZTO thick film formed by AD are compared in Fig. 1(d). The calculated patterns for P2-type NZTO phase based on their structure data are also plotted as the references [1, 2]. The peak positions for both ball-milled NZTO powder and NZTO

thick film formed by AD well agree with the calculated pattern, while the peaks in thick film become slightly broader compared to powder sample. For example, the full width at half maximum (FWHM) for the peak from 002 plane is 0.18° for ball-milled powder and 0.24° for as-deposited film, respectively. This would be caused by the degradation of the crystallinity of NZTO by plastic deformation and/or fracturing of NZTO particles during the impact consolidation [10–15].

Fig. 2 shows the Bode plot and Nyquist plot of the complex impedance ($Z' + jZ''$) at room temperature for a NZTO thick film formed on a SUS316L substrate. Before the measurement, Au film electrode with the area size of 0.5 cm^2 was formed by sputtering, and both an Au film and a SUS316L substrate behave as the ion blocking electrodes for ionic conduction [13, 15]. The Nyquist plot is composed of the part of a distorted semicircle at frequency above 10 kHz and a linear tail at low frequency range. These data belong to the ionic conduction at NZTO grain boundaries and the response by ionic blocking electrodes, respectively [4, 5]. Since the upper limit of measurement frequency was 3 MHz, the data reflecting the ionic conduction in NZTO grain is not observed clearly. The solid line in Fig. 2(b) represents the fitting curve for the equivalent circuit consisting of $(R_b)(R_{gb}-Q_{gb})(Q_{el})$, where R_b , R_{gb} , Q_{gb} and Q_{el} correspond to the bulk resistance, grain-boundary resistance, constant phase angle element (CPE) of grain boundary and CPE of electrodes. Suppression degree α of $(R_{gb}-Q_{gb})$ circuit was calculated to be 0.57. Consequently, the value of R_b , R_{gb} and Q_{gb} for NZTO film are estimated to be $66 \Omega \text{ cm}^2$, $271 \Omega \text{ cm}^2$ and $0.27 \times 10^{-8} \text{ F}$, respectively.

The total resistance $R_{\text{total}} = R_b + R_{gb}$ for ionic conduction of NZTO thick film is calculated to be $337 \Omega \text{ cm}^2$, resulting into total ionic conductivity σ_{total} of $0.74 \times 10^{-5} \text{ S cm}^{-1}$ at room temperature, which is slightly higher than as-deposited Li ion conducting ceramic films formed by AD [12–15]. Since $R_{gb} / R_{\text{total}}$ is approximately 0.80, bulk conductivity is well above $1 \times 10^{-5} \text{ S cm}^{-1}$ at room temperature. Although σ_{total} of as-deposited NZTO film is approximately two order lower than the conductivity of sintered NZTO [2–5], but approximately 2–3 times higher than amorphous LiPON film used as a solid electrolyte in thin film Li battery [16]. We believe that the lower conductivity of NZTO thick film formed by AD compared to sintered NZTO is attributed to both low relative density and higher density of grain boundary in AD film. Fig. 3 shows the measurement result for potentiostatic polarization current at room temperature and applied DC voltage of 20 mV for a NZTO thick film formed on a SUS316L substrate. As can be seen, the output current is almost saturated at approximately 2 nA, corresponding to the area specific resistance for

electronic conduction of $5 \times 10^6 \Omega \text{ cm}^2$. The electronic conductivity σ_e of NZTO thick film is calculated to be $0.5 \times 10^{-9} \text{ S cm}^{-1}$, which is approximately four orders lower than ionic conductivity σ_{total} as mentioned above. Consequently, ionic transfer number ($= \sigma_{\text{total}} / (\sigma_{\text{total}} + \sigma_e)$) is estimated to be 0.99993, indicating the dominant Na ion conduction of NZTO thick film.

Reducing the film thickness is simple and effective way to reduce the area specific resistance for ionic conduction. Thinner NZTO film with the thickness of approximately $4 \mu\text{m}$ (Fig. S1 in supplemental data) can be fabricated easily by shortening the processing time for AD, but when Au film was coated on the surface of thin NZTO film by sputtering, soft-short occurred between Au film and SUS316L substrate due to the low film density. To achieve both higher Na ion conductivity and good insulating property for electron conduction for as-deposited NZTO film formed by AD, further study is necessary to increasing the film density by controlling the size and morphology of NZTO base powder.

4. Conclusion

NZTO thick films were successfully fabricated by AD method without applying any thermal treatment. Obtained thick film formed by AD has a thickness of $25 \mu\text{m}$ and an identical crystal structure with base powder. Ionic conductivity of as-deposited NZTO thick film was estimated to be $0.74 \times 10^{-5} \text{ S cm}^{-1}$ at room temperature, while electronic conductivity of the film was four orders of magnitude lower than the ionic conductivity. Although the ionic conductivity of as-deposited NZTO film by AD is more than one order of magnitude lower than that of sintered NZTO, obtained electrical conducting property could be applicable for solid electrolyte layer in a thin film sodium-ion battery.

Acknowledgements

This work was partly supported by Grant-in-Aid for Scientific Research (JSPS KAKENHI) Grant Number 22H01468 from the Japan Society for the promotion of Science (JSPS) and Foundation of Public Interest of Tatematsu, Japan.

References

- [1] M.A. Evstigneeva, V.B. Nalbandyan, A.A. Petrenko, B.S. Medvedev, A.A. Kataev, *Chem. Mater.* 23 (2011) 1174–1181.

- [2] Y. Li, Z. Deng, J. Peng, E. Chen, Y. Yu, X. Li, J. Luo, Y-Y. Huang, J. Zhu, C. Fang, Q. Li, J. Han, *Chem. Eur. J.* 24 (2018) 1057–1061.
- [3] J-F. Wu, Q. Wang, X. Guo, *J. Power Sources* 402 (2018) 513–518.
- [4] A. Itaya, K. Yamamoto, R. Inada, *Mater. Lett.* 284 (2021) 128941.
- [5] A. Itaya, K. Yamamoto, R. Inada, *Int. J. Appl. Ceram. Technol.* 18 (2021) 2085–2090.
- [6] G.E. Youngblood, G.R. Miller, R.S. Gordon, *J. Am. Ceram. Soc.* 61 (1978) 86–87.
- [7] X. Lu, G. Xia, J.P. Lemmon, Z. Yang, *J. Power Sources* 195 (2010) 2431–2442.
- [8] J.B. Goodenough, H.Y-P. Hong, J.A. Kafalas, *Mater. Res. Bull.* 11 (1976) 203–220.
- [9] Q. Ma, C-L. Tsai, X-K. Wei, M. Heggen, F. Tietz, J.T.S. Irvine, *J. Mater. Chem. A* 7 (2019) 7766–7776.
- [10] J. Akedo, *J. Therm. Spray Technol.* 17 (2008) 181–198.
- [11] D. Hanft, J. Exner, M. Schubert, S. Thomas, P. Fuierer, R. Moos, *J. Ceram. Sci. Technol.* 6 (2015) 147–182.
- [12] D. Popovici, H. Nagai, S. Fujishima, J. Akedo, *J. Am. Ceram. Soc.* 94 (2011) 3847–3850.
- [13] R. Inada, K. Ishida, M. Tojo, T. Okada, T. Tojo, Y. Sakurai, *Ceram. Internat.* 41 (2015) 11136–11142.
- [14] D. Hanft, J. Exner, R. Moos, *J. Power Sources* 361 (2017) 61–69.
- [15] R. Inada, T. Okada, A. Bando, T. Tojo, Y. Sakurai, *Prog. Nat. Sci. Mater. Internat.* 27 (2017) 350–355.
- [16] J.B. Bates, N.J. Dudney, B. Neudecker, A. Ueda, C.D. Evans, *Solid State Ionics* 135 (2000) 33–45

Table 1. Parameters for NZTO film fabrication by AD.

Substrate material	SUS316L (thickness = 0.5 mm)
Orifice size of nozzle	10 mm × 0.5 mm
Distance between a substrate and a nozzle	10 mm
Scan speed of a substrate	10 mm s ⁻¹
Scan length of a substrate	50 mm
Mass flow of N ₂ career gas	10 L min ⁻¹
Pressure of deposition chamber without career gas	50 Pa
Mass of NZTO powder set in aerosol chamber	1.5 g
Duration time for deposition	10 min

Figures with captions

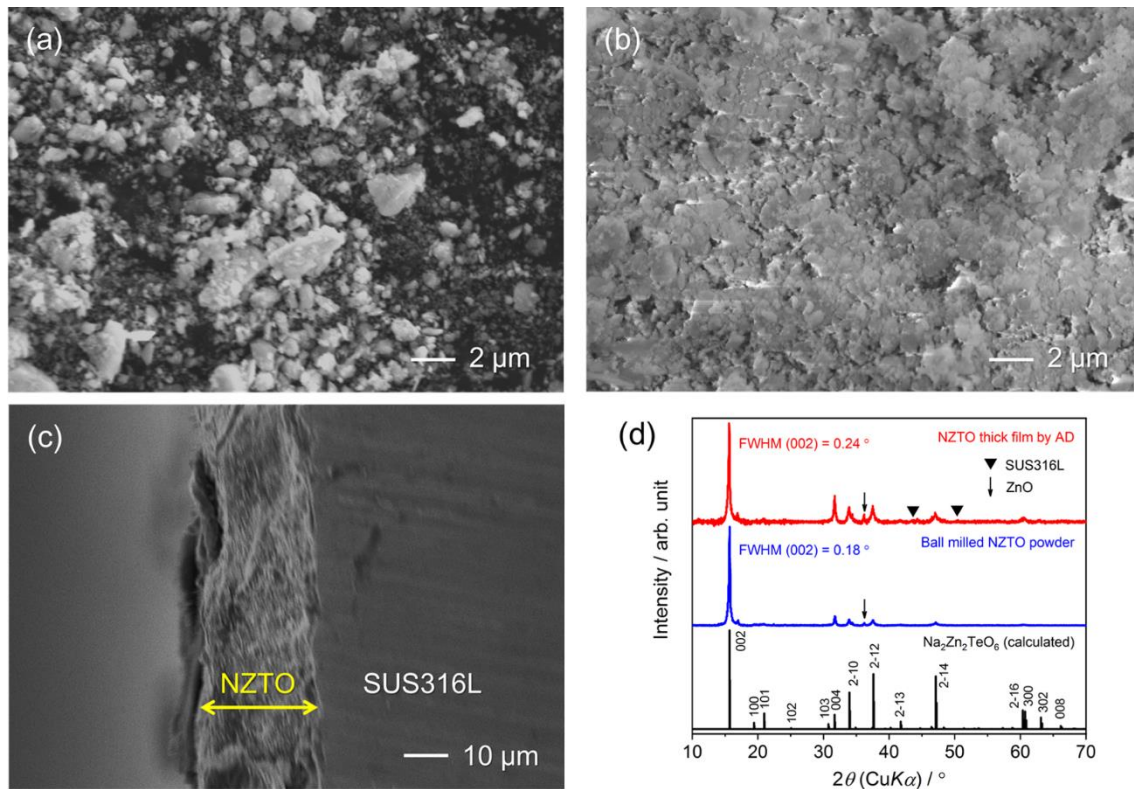


Fig. 1. SEM images for (a) ball-milled NZTO powder used for film fabrication, (b) the surface and (c) transverse cross section of NZTO thick film formed by AD. XRD patterns for NZTO powder and thick film are compared in (d).

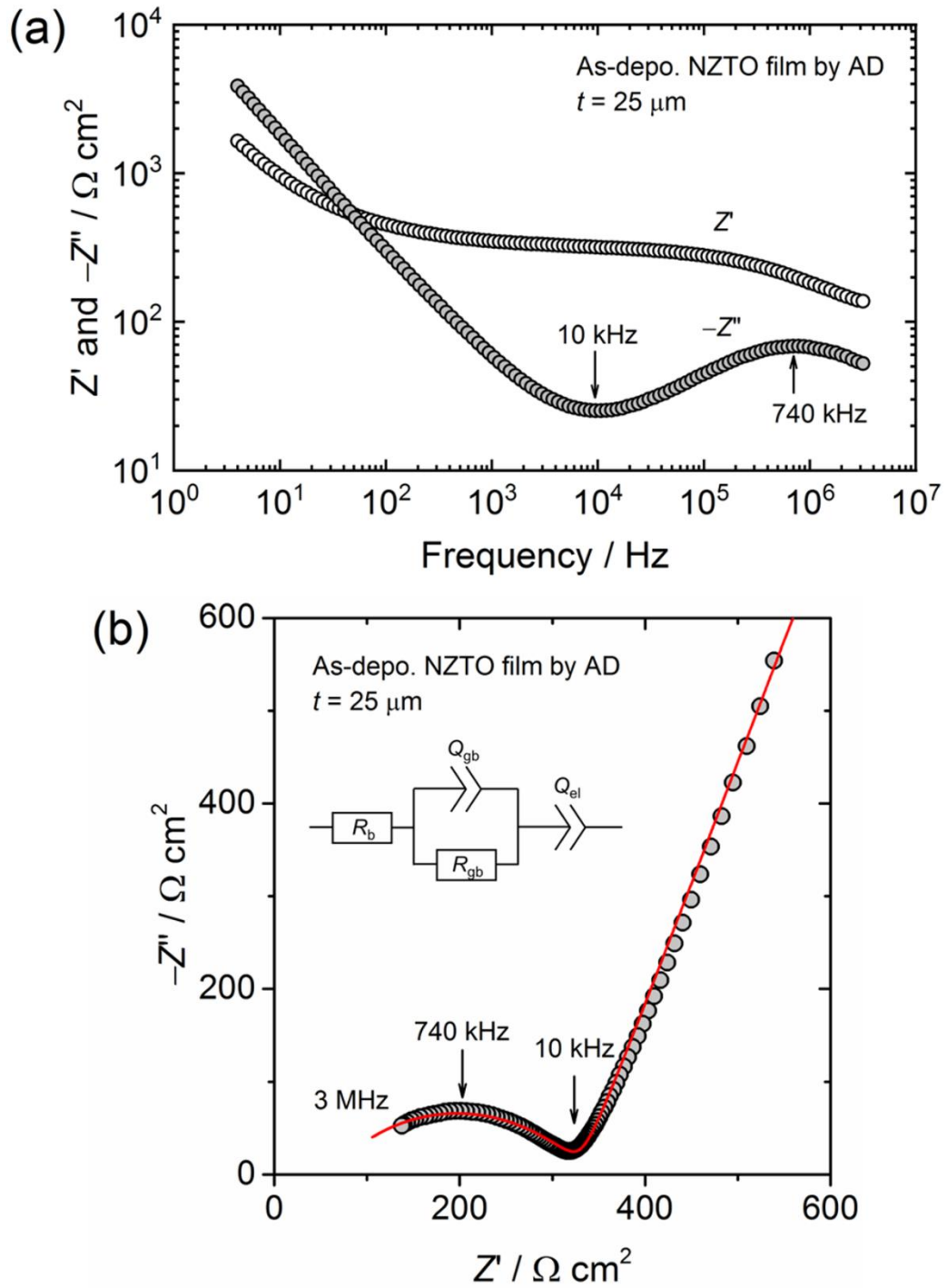


Fig. 2. (a) Bode plot and (b) Nyquist plot of complex impedance measured at 27°C for NZTO thick film.

The solid line in (b) are the fitting curve by the equivalent circuit (inset).

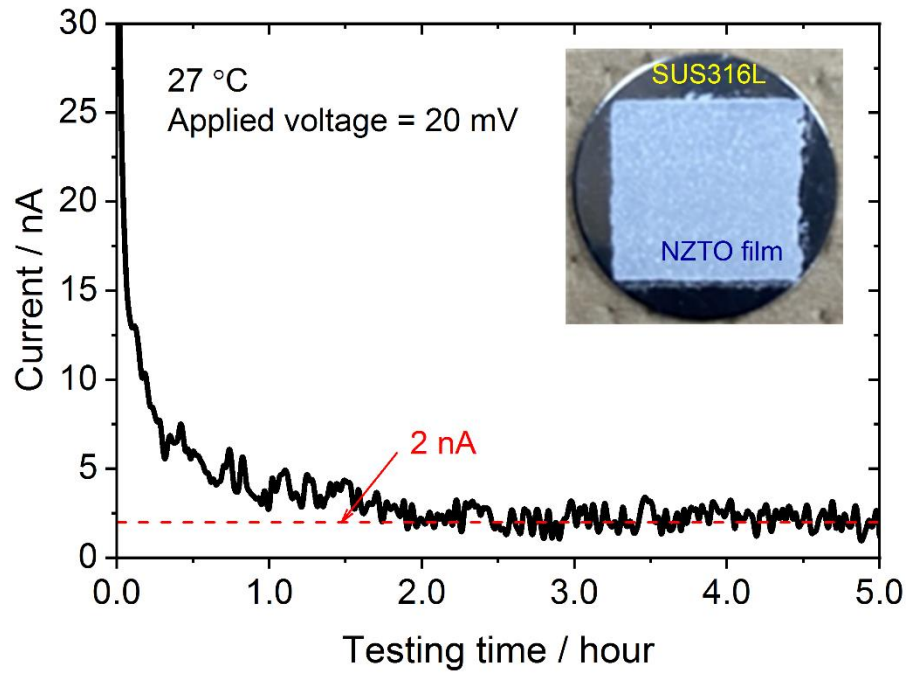


Fig. 3. Potentiostatic polarization current as a function of measuring time at 27 °C and 20 mV for NZTO thick film. Inset is the photo of NZTO thick film on a SUS316L substrate.